Time-Frequency Characteristics and PAPR Reduction of OTDM Waveform for 5G and Beyond

Jehad M. Hamamreh* and Huseyin Arslan*§
*School of Engineering and Natural Sciences, Istanbul Medipol University, Istanbul, Turkey, 34810
§Department of Electrical Engineering, University of South Florida, Tampa, FL, 33620

***Abstract*—This paper provides an in-depth investigation and analysis on the characteristics of channel-based transform waveforms and their differences from Fourier transform-based waveforms. Particularly, the basis functions of the recently proposed orthogonal transform division multiplexing (OTDM) waveform, which belongs to the category of channel-based transform waveforms, are comprehensively compared with the fixed exponential basis functions of orthogonal frequency division multiplexing (OFDM) waveform, which pertains to the class of Fourier transform-based waveforms. The obtained results show significant differences in the time and frequency characteristics of both classes of the waveforms. Also, the peak-to-average power ratio (PAPR) of OTDM is investigated and compared to OFDM. Then, a new effective technique, referred to as OTDM with edge subcarrier dedication (OTDM-ESD), is proposed for PAPR reduction by exploiting the special characteristics of the effective channel response in OTDM waveform. Simulation results show that the proposed OTDM-ESD technique not only reduces the PAPR, but also enhances the BER performance significantly.**

I. Introduction

OFDM has been the most dominantly used transmission scheme in the vast majority of the current broadband systems, such as LTE, WiFi and DVT. It has been adopted due to its desirable features, including higher spectral efficiency, simple equalization in the frequency domain, easy integration with MIMO systems and multi-user diversity, with the ability to flexibly schedule both time and frequency resources among users [1]. Nonetheless, OFDM has several major drawbacks, such as high peak-to-average power ratio (PAPR), spectral leakage, strict synchronization requirement and frequency offset sensitivity. Moreover, OFDM is proven to be a non-optimal transceiver design in terms of overall performance, and also lacks physical layer security features [2], which are very desirable in future 5G and beyond systems, making it inherently vulnerable to eavesdropping. Due to the aforementioned shortcomings, there has been a global consensus on the incapability of OFDM alone in satisfying all the needs of future networks and their diverse expected applications, such as Tactile Internet, Machine to Machine (M2M) and Internet of Thing (IoT) [3]. Thus, researchers around the world have been trying to design new waveforms or different numerologies of OFDM to meet the requirements of future emerging 5G-enabled applications and scenarios [3].

In the literature [4] [5], many waveforms have been proposed to address some of the OFDM drawbacks. Among these are filtered-OFDM, windowed-OFDM, FBMC, UW-OFDM, GFDM, UFMC, ZT-DFT-s-OFDM, UW-DFT-s-OFDM, etc.

As inferred from the literature, most of the recently proposed waveforms for 5G systems are Fourier transform-dependent and designed without taking channel realizations into account. This kind of design comes with two major demerits. Firstly, it results in a non-optimal transceiver design, where the transmit and receive basis functions (pulses) are static and do not adapt to the channel variations. Secondly, it is vulnerable to wireless eavesdropping, where physical layer security has not been considered as a requirement in the aforementioned waveform designs. To address these problems, the authors in [2] proposed an adaptive channel-based transform waveform, called orthogonal transform division multiplexing (OTDM), for future secure 5G and beyond systems. In particular, instead of using fixed exponential basis functions, produced by IFFT and FFT as in OFDM, new orthogonal basis functions are extracted from the channel and used to securely modulate and demodulate the data symbols at the transmitter and receiver sides, respectively. This design results in two major merits over the currently existing waveforms in the literature. First, it provides physical layer security, a new important feature, which comes for free as a result of the channel-based design. Second, it enhances reliability and robustness against channel impairments, where better BER performance is obtained as a result of increasing the effective signal-to-noise ratio (SNR). The waveform design reported in [2] was presented from a pure security perspective, where the mathematical framework of the design was introduced and its immunity against eavesdropping was proven. However, the time-frequency characteristics of the basis functions of OTDM as well as its PAPR and their differences from OFDM were not investigated. Therefore, this paper comes to complement and build on top of the work presented in [2] to address the aforementioned issues. Specifically, we make the following main contributions:

- We investigate and visualize the time and frequency characteristics of the basis functions of OTDM waveform, and show how their shapes vary for different channel realizations. Then, we exhibit their differences from the complex exponential basis functions of OFDM-based waveforms. This is performed in order to provide insights and an in depth understanding of the concept of channel-based transform waveforms.
- We examine the PAPR of OTDM and demonstrate how its distribution is the same as that of OFDM. Thus, this

motivates finding an efficient PAPR reduction technique, specifically designed for OTDM waveform.
- By exploiting the fact that the deep-faded subchannels of the effective channel transform response in OTDM waveform are always localized and situated at the left edge of the OTDM block, we propose an effective method that exploits this feature for reducing its PAPR.

The rest of the paper is organized as follows. The system model is described in Section II. The OTDM waveform characteristics and their differences from OFDM are exhibited in Section III. The details of the proposed PAPR reduction technique for OTDM are revealed in Section IV. Simulation results are discussed in Section V. Finally, a concise conclusion is drawn in Section VI.[1]

II. Preliminaries and System Model

A single-input single-output (SISO) system, in which a transmitter (Tx), called Alice, is communicating with a legitimate receiver (Rx), called Bob, whereas an eavesdropper, called Eve, is trying to intercept the communication between the two legitimate parties (Alice and Bob). All received signals experience independent multi-path slowly varying Rayleigh fading channels [2]. Also, the channel reciprocity property is adopted, where the downlink channel can be estimated from the uplink one, in a time division duplex (TDD) system [6].

In the OTDM waveform design [2], channel-based transform basis functions are used as subcarriers for the complex baseband modulated symbols, s_i. The total number of data symbols in one transmission block $\mathbf{s} = \begin{bmatrix} s_0 & s_1 & ... & s_{N-1} \end{bmatrix}^{\mathrm{T}}$ is N. Each of s_i is carried by a specific channel-based orthogonal pulse $\mathbf{v} \in \mathbb{C}^{[N\times 1]}$, where the mapping process in this case is basically implemented via a simple multiplication operation between each data symbol and an orthogonal basis function. For the N data symbols to be transmitted, we need N carrying orthogonal basis functions, which can be taken from the column vectors of $\mathbf{V}$, given by

$$\mathbf{V} \;=\; \begin{bmatrix} \mathbf{v}_0 & \mathbf{v}_1 & ... & \mathbf{v}_{N-1} \end{bmatrix} \in \mathbb{C}^{[N\times N]}. \tag{1}$$

Hence, $\mathbf{V}$ can be seen as the channel-based transform matrix, which can be obtained by decomposing the channel matrix $\mathbf{H_b} \in \mathbb{C}^{[(N+L-1)\times N]}$ of the legitimate user's channel impulse response $\mathbf{h_b} = \begin{bmatrix} h_0 & h_1 & ... & h_{L-1} \end{bmatrix}^{\mathrm{T}}$ using SVD as follows

$$\mathbf{H_b} = \mathbf{U}\mathbf{E}\mathbf{V}^{\mathrm{H}}. \tag{2}$$

Note that $\mathbf{H_b}$ is an $(N + L - 1) \times N$ Toeplitz matrix with first column $\begin{bmatrix} h_0 & h_1 & \cdots & h_{L-1} & 0 & \cdots & 0 \end{bmatrix}^{\mathrm{T}}$ and first row $\begin{bmatrix} h_0 & 0 & \cdots & 0 \end{bmatrix}^{\mathrm{T}}$. Each ith column (basis function) in $\mathbf{V}$ can be expressed as $\mathbf{v_i} = \begin{bmatrix} v_0 & v_1 & ... & v_{N-1} \end{bmatrix}^{\mathrm{T}}$. After multiplying each symbol with its corresponding basis function, we multiplex and sum all the resulting vectors to get a block of samples, $\mathbf{x}$, referred to as one OTDM symbol. This process can mathematically be stated as

$$\mathbf{x} \;=\; \sum_{i=0}^{N-1} s_i \mathbf{v}_i, \in \mathbb{C}^{[N\times 1]}, \tag{3}$$

which can further be simplified into a matrix form as

$$\mathbf{x} \;=\; \mathbf{V}\mathbf{s} \in \mathbb{C}^{[N\times 1]}. \tag{4}$$

From a signal processing point of view, this looks similar to transmit pre-coding in spatial multiplexing MIMO, but here the matrix is extracted from the temporal (not spatial) variation of the channel. To avoid the inter-block interference (IBI), zero-padding (ZP) as a guard interval of length $L - 1$, is appended to the end of each block. After OTDM block, $\mathbf{x}$, is sent through the channel, the received signal at Bob can be given as

$$\mathbf{y} \;=\; \mathbf{h_b} \circledast \mathbf{x} + \mathbf{z_b}, \tag{5}$$

$$y_i \;=\; \sum_{l=0}^{L-1} h_l x_{(i-l)} + z_{b(i)}, \tag{6}$$

where $\mathbf{y} = \begin{bmatrix} y_0 & y_1 & ... & y_{N+L-1} \end{bmatrix}^{\mathrm{T}}$ is the received block of one OTDM symbol and $\mathbf{z_b} \in \mathbb{C}^{[(N+L-1)\times 1]}$ is the zero-mean complex additive white Gaussian noise (AWGN) at Bob. The previous convolution form can also be equivalently written in a linear algebraic matrix form as

$$\mathbf{y} \;=\; \mathbf{H_b}\mathbf{x} + \mathbf{z_b} = \mathbf{H_b}\mathbf{V}\mathbf{s} + \mathbf{z_b} = \mathbf{U}\mathbf{E}\mathbf{s} + \mathbf{z}. \tag{7}$$

To remove the effect of the time dispersion caused by the channel spread at the Rx, a channel-based transformation process is performed on $\mathbf{y}$ using matrix $\mathbf{U}^H = \begin{bmatrix} \mathbf{u}_1^* & \mathbf{u}_2^* & \cdots & \mathbf{u}_{N+L-1}^* \end{bmatrix} \in \mathbb{C}^{[N\times(N+L-1)]}$. Each ith column (basis function) in $\mathbf{U}^{\mathrm{H}}$ can be expressed as $\mathbf{u}_i^* = \begin{bmatrix} u_0 & u_1 & ... & u_{N-1} \end{bmatrix}^{\mathrm{T}}$. The matrix $\mathbf{U}^{\mathrm{H}}$ consists of multiple orthogonal basis functions, which are optimally extracted from the channel and can be used as inverse basis functions to extract the transmitted block by diagonalizing the channel response. To do so, the Rx transforms $\mathbf{y}$ using $\mathbf{U}^{\mathrm{H}}$ as follows:

$$\sum_{i=0}^{N+L-1} y_i \mathbf{u}_i^* \;=\; \mathbf{U}^{\mathrm{H}}\mathbf{y} = \mathbf{E}\mathbf{s} + \mathbf{U}^{\mathrm{H}}\mathbf{z} = \mathbf{E}\mathbf{s} + \hat{\mathbf{z}}, \tag{8}$$

where $\hat{\mathbf{z}} = \mathbf{U}^{\mathrm{H}}\mathbf{z} \in \mathbb{C}^{[N\times 1]}$. It should be noted that the vectors of $\mathbf{U}^{\mathrm{H}}$ span not only the whole transmitted block time but also the following time reserved for ZP. After multiplying by $\mathbf{U}^{\mathrm{H}}$, the leakage energy of the signal due to channel spreading will be collected from the ZP optimally with minimal noise thanks to the optimal extracted basis functions, whose length at the Rx is equal to the received OTDM signal's length. The estimated data symbols can be obtained by equalizing the effect of the diagonal matrix $\mathbf{E} \in \mathbb{C}^{[N\times N]}$, which contains the channel gain over each data symbol. Thus, the final equalized block of data symbols $\tilde{\mathbf{s}}$ can be obtained by performing simple one tap equalization in the transform domain as given below

$$\tilde{\mathbf{s}} \;=\; \mathbf{E}^{-1}\mathbf{U}^{\mathrm{H}}\mathbf{y} = \mathbf{E}^{-1}\left(\mathbf{E}\mathbf{s} + \mathbf{U}^{\mathrm{H}}\mathbf{z}\right) \tag{9}$$

$$\;=\; \mathbf{s} + \mathbf{E}^{-1}\mathbf{U}^{\mathrm{H}}\mathbf{z} = \mathbf{s} + \mathbf{E}^{-1}\hat{\mathbf{z}}. \tag{10}$$

[1] Notations: In this paper, vectors are denoted by bold-small letters, whereas matrices are denoted by bold-capital letters. $\mathbf{I}$ is the $N \times N$ identity matrix. Norm-2 and norm-infinity are defined by $\|\cdot\|_2$ and $\|\cdot\|_\infty$, respectively. The convolution, inverse, transpose and conjugate transpose operators are symbolized by ($\circledast$), $(\,\cdot\,)^{-1}$, $(\,\cdot\,)^{\mathrm{T}}$ and $(\,\cdot\,)^{\mathrm{H}}$, respectively.

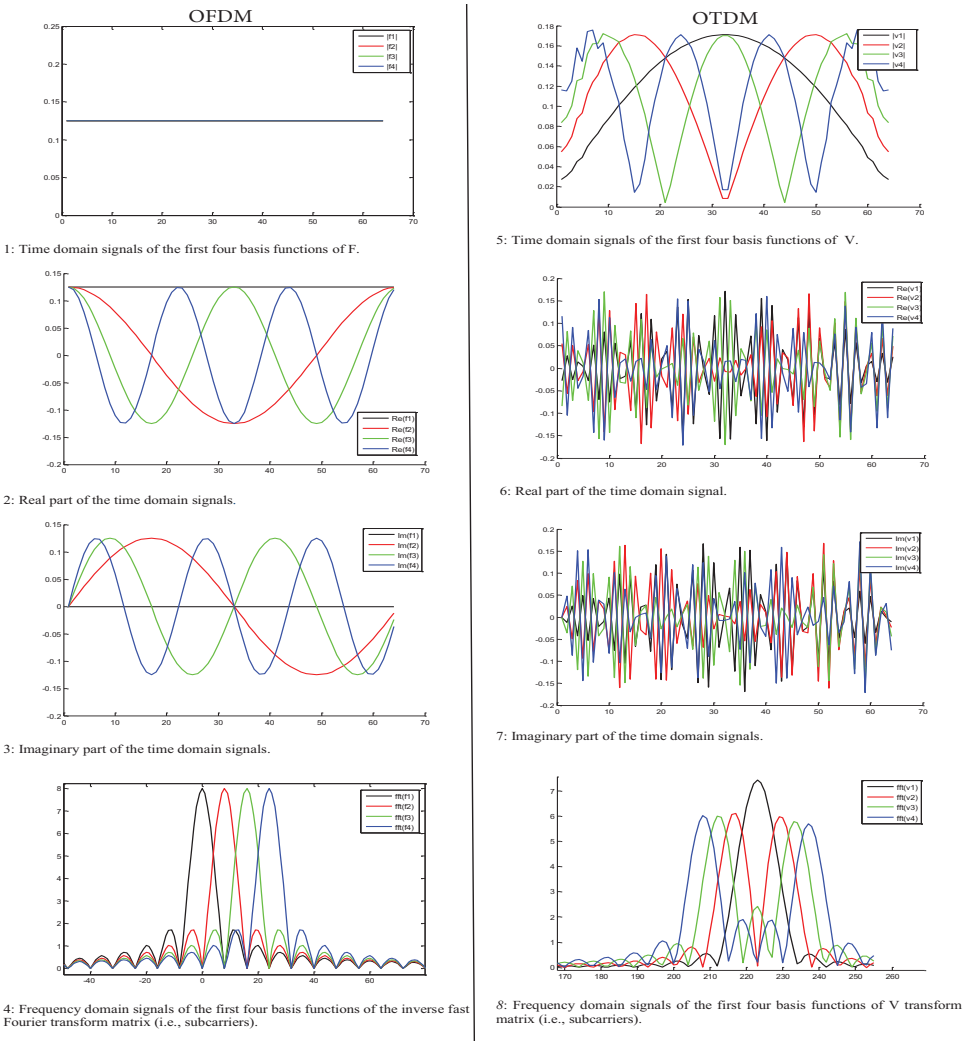

Fig. 1. Waveform comparison between OFDM and OTDM in terms of the: 1) amplitude, 2) real part, 3) imaginary part, and 4) frequency shapes of the first four basis functions of the inverse Fourier and channel-based transform matrices given by $\mathbf{F}^{\mathrm{H}}$ and $\mathbf{V}$ (extracted from a channel with $L = 9$ taps), respectively.

III. Waveform Characteristics: OTDM vs OFDM

In most of the previously developed multi-carrier transmission methods, the orthogonal sub-carriers (basis functions), which are generated by IFFT and FFT at the Tx and Rx sides, respectively, are fixed and channel-independent. This design results in a static, channel-unaware, non-optimal, and insecure transmission. However, in the channel-based transform design, the orthogonal basis functions, on which the symbols are carried on, are directly extracted from the small scale multi-path channel and used at both the Tx and Rx to optimally diagonalize the channel. Here, we provide an in-depth investigation and comparison of the waveform shapes and time-frequency characteristics between channel-based transform and Fourier-based transform waveforms. Particularly, we pick OTDM as a waveform that represents channel-based transform waveform class and OFDM as another waveform that represents Fourier-based transform waveform class. Fig. 1 shows the major differences between the shape of the pulses in time and frequency domains of OFDM and OTDM waveforms. It is observed that for a certain channel response the time domain shapes of the basis functions in OTDM are multiple of half cosine pulses compared to fixed rectangular pulses in OFDM. Consequently, the frequency domain shapes of the basis functions in OTDM are different from OTDM as visualized in Fig. 1. On the other hand, Fig. 2 describes how the time and spectral shapes of the pulses change for different channel realizations. This explains the adaptivity and security nature of OTDM and how it adopts to changing channels. Fig. 3 presents the effective channel transform response of OTDM obtained by $\mathbf{E}$ (on the left part of the figure), and its difference from the channel frequency response of OFDM (on the right part of the figure). As depicted, the subchannel gains in OTDM waveform are sorted in a descending order, and thus the deep-faded subchannels are localized at the edge of the effective channel transform response. This special feature will be exploited to design a channel-dependent PAPR reduction technique, as it will be explained in the next Section. On the contrary, the subchannel gains in OFDM waveform are not-sorted and the deep-faded

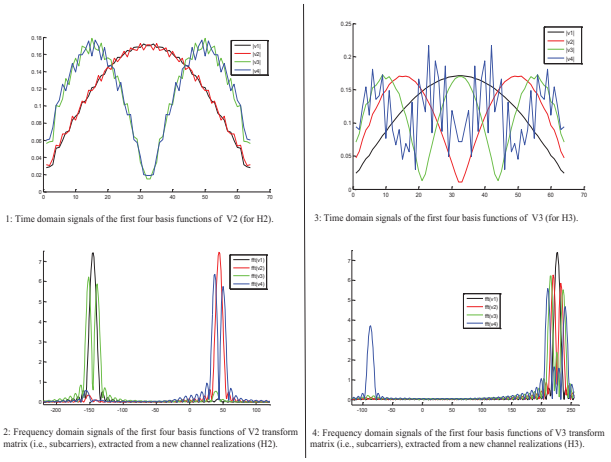

Fig. 2. Time-frequency characteristics of the first four basis functions for two different channel realizations with $L = 9$ exponentially decaying taps.

subchannels are distributed over the whole channel frequency response.

IV. OTDM with Edge Subcarrier Dedication (OTDM-ESD): PAPR Reduction Technique

Many techniques have been proposed in the literature to reduce the PAPR of OFDM waveform [7]. However, the direct implementation of these techniques on OTDM waveform will not be efficient and optimal in terms of the overall system performance. This is due to the fact that the OTDM characteristics are different from those of OFDM. Thus, by taking advantage of the inherent nature of OTDM, a more effective PAPR reduction technique can be devised. Here, we propose an efficient channel-dependent tone reservation (TR) technique to specifically reduce the PAPR of OTDM waveforms. The key idea is to exploit the inherent characteristics of the channel transform response of OTDM (shown in Fig. 3) in order to design a technique that not only reduces the PAPR, but also enhances the reliability performance, which is different from the conventional TR technique [7], in which the reserved subcarriers are not channel dependent. Particularly, the fact that deep-faded subchannels in OTDM are always localized at the edge of the effective channel response enables us to simply determine the number of subcarriers that are required to be used for PAPR reduction, and then assign the contiguous edge sub-carriers corresponding to the deep-faded subchannels for PAPR reduction. Without loss of generality, in this method, we partition the OTDM block into two parts, in which the first part, which corresponds to good subchannels, is dedicated and used for data tranmission; while the second part, which corresponds to the deep-faded (bad) subchannels located at the edge of each OTDM block, is dedicated for PAPR reduction. By doing so, we ensure minimum capacity reduction as those subcarriers used for PAPR are already not good to be used for data transmission. Unlike the classical TR technique, a prior knowledge on the positions of the subcarriers used for PAPR reduction is not needed. In the proposed design, the

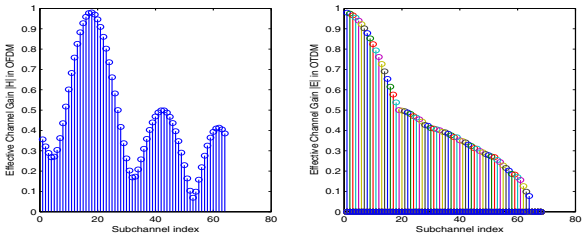

Fig. 3. Comparison between the effective channel transform responses of OFDM (left shape) and OTDM (right shape).

transmitted signal can be modeled as

$$\mathbf{d} = \mathbf{GV}[\mathbf{s}\ \mathbf{w}]^{\mathrm{T}} \in \mathbb{C}^{[(N+L-1)\times 1]}, \tag{11}$$

where $\mathbf{s} \in \mathbb{C}^{[1\times(N-R)]}$ is a set of QAM symbols contained in a vector, $\mathbf{w} \in \mathbb{C}^{[1\times R]}$ is a set of samples to be optimized to reduce PAPR, $\mathbf{V}$ is the N-point channel-based transformation matrix, and $\mathbf{G} \in \mathbb{C}^{[(N+L-1)\times N]}$ is the ZP addition matrix. The PAPR of the above-transmitted signal is the ratio of the maximum transmitted power to the average power, which can be given as

$$PAPR = \frac{\|\mathbf{GV}([\mathbf{s}\ \mathbf{w}]^{\mathrm{T}})\|_{\infty}^{2}}{\frac{1}{N+L-1}\|\mathbf{GV}([\mathbf{s}\ \mathbf{w}]^{\mathrm{T}})\|_{2}^{2}}. \tag{12}$$

The problem here reduces to finding the optimal AN vector $\mathbf{w}$ that can effectively reduce the PAPR of the signal $\mathbf{d}$. Thus, the optimization problem to be solved can be formulated as

$$\begin{aligned} \mathbf{w}_{opt} &= \arg\ \min_{\mathbf{w}} \|\mathbf{GV}([\mathbf{s}\ \mathbf{w}]^{\mathrm{T}})\|_{\infty}^{2} \\ &subject\ to \rightarrow \|\mathbf{w}\|_{2}^{2} \leq \lambda \times \|\mathbf{s}\|_{2}^{2}, \end{aligned} \tag{13}$$

where the percentage of power used by $\mathbf{w}$ signal is controlled by λ. The objective function shows that we have a convex optimization problem that can numerically be solved by some advanced and powerful convex optimization solvers such as MOSEK. In this case, to obtain a precise numerical solution to the optimization problem in our hands, we adopt using YALMIP, a handy optimization package that can be integrated with MOSEK and MATLAB to solve complex problems.

V. Simulation Results

In this section, we provide simulation results to demonstrate the effectiveness of the proposed OTDM-ESD technique in reducing the PAPR and enhancing the BER performance as well as its performance comparison with OTDM and OFDM waveforms. We consider an OTDM system with $N = 64$ modulated QPSK data symbols and a guard period of length L. The channel is modeled as an independent and identically distributed (i.i.d.) block-fading, where channel coefficients are drawn according to an i.i.d. Rayleigh fading distribution at the beginning of each block transmission, and remain constant within one block, but change independently from one to another. The Rayleigh multi-path fading channel has nine taps $L = 9$ with an exponential power delay profile. Additionally, we assume an eavesdropper, who uses its channel to extract

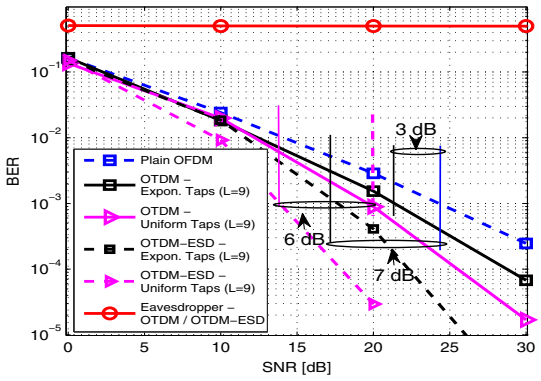

Fig. 4. BER comparison of OTDM-ESD with OTDM and OFDM.

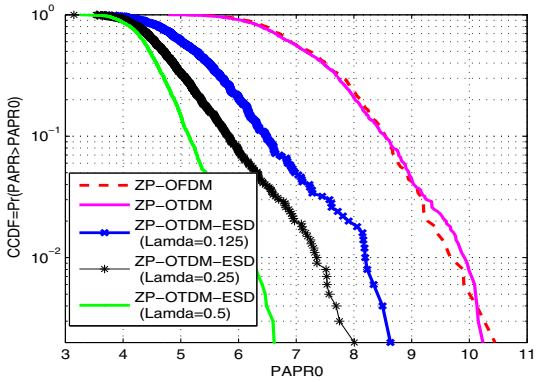

Fig. 5. PAPR comparison of OTDM-ESD with OTDM and OFDM.

its basis functions, trying to intercept the communication. For the sake of fair comparison, we also consider a standard OFDM system with $N = 64$ active sub-carriers and a cyclic prefix (CP) of length L. Fig. 4 shows the bit error rate (BER) performance gain of a legitimate Rx, employing OTDM waveform compared to OFDM using the same parameters. It is shown that OTDM outperforms OFDM by at least 3 dB at BER=10^{-3} and that the gain increases as the SNR increases. This gain is obtained as a result of not discarding the leaked energy, but instead collecting it optimally by adopting the shape and length of the receive orthogonal basis functions according to the channel spread, in such a way that the total response of the system is diagonalized. Fig. 4 also presents the BER enhancement delivered by the OTDM-ESD technique for PAPR reduction. It is shown that there is around 4 dB gain compared to OTDM, and around 7 dB gain compared to OFDM. The resulting gain is due to dedicating the right edge sub-carriers corresponding to the deep-faded subchannels for PAPR reduction, instead of using them for data transmission. In other words, the gain is obtained as a result of avoiding the usage of the low subchannel gains that are responsible for limiting the system performance; instead, they are used for PAPR reduction and then discarded at the Rx.

Moreover, it is shown that the gain of a uniformly distributed power delay profile is more than that of a channel with exponentially distributed power delay profile. This is because uniform profile has equally significant spreading gain over all taps, while exponential profile has an insignificant gain at most of its high ordered taps due to its fast decaying nature. Thus, the accumulated energy from the ZP period in the case of uniform profile is higher than that of the exponential profile, resulting in a much lower BER. Additionally, Fig. 4 depicts the very bad BER performance of Eve although she is assumed to be fully aware of the method. This happens due to the use of channel-dependent waveforms through Alice-to-Bob channel, which are different from Alice-to-Eve channel. Thus, the system response will not be diagonalized for Eve. This will results in a severe inter-symbol interference between data symbols with respect to Eve. Fig. 5 explicitly shows that the PAPR of OTDM is the same as that of OFDM because both waveforms represent multi-carrier block based transmission schemes. However, when the proposed OTDM-ESD technique is applied by reserving only 8 subcarriers as peak reduction tones, significant PAPR reduction gain is achieved. Also, it is observed that the PAPR reduction gets better as the power of the peak reduction tones increases. These results prove the benefits of OTDM-ESD.

VI. Conclusion

In this paper, we have investigated the characteristics of a new candidate 5G waveform, called OTDM. For this purpose, we have provided thorough comparison between OTDM and OFDM. Particularly, we presented the time and frequency domain shapes of its basis functions (pulses), which are extracted from the wireless channel, and showed how they change for different channel realizations. Moreover, we have examined the PAPR performance of OTDM compared to OFDM, and then presented an effective technique for reducing it.

Acknowledgment

This work is supported by The Scientific and Research Council of Turkey (TUBITAK) under grant No. 114E244.

References

[1] A. A. Zaidi, R. Baldemair, H. Tullberg, H. Bjorkegren, L. Sundstrom, J. Medbo, C. Kilinc, and I. D. Silva, "Waveform and Numerology to Support 5G Services and Requirements," *IEEE Commun. Mag.*, vol. 54, no. 11, pp. 90–98, November 2016.

[2] J. M. Hamamreh and H. Arslan, "Secure Orthogonal Transform Division Multiplexing (OTDM) Waveform for 5G and Beyond," *IEEE Communications Letters*, vol. 21, no. 5, pp. 1191–1194, May 2017.

[3] Z. ANKARALI, B. Pekoz, and H. ARSLAN, "Flexible Radio Access Beyond 5G: A Future Projection on Waveform, Numerology Frame Design Principles," *IEEE Access*, vol. PP, no. 99, pp. 1–1, 2017.

[4] X. Zhang, L. Chen, J. Qiu, and J. Abdoli, "On the Waveform for 5G," *IEEE Commun. Mag.*, vol. 54, no. 11, pp. 74–80, November 2016.

[5] A. Sahin, R. Yang, E. Bala, M. C. Beluri, and R. L. Olesen, "Flexible DFT-S-OFDM: Solutions and Challenges," *IEEE Commun. Mag.*, vol. 54, no. 11, pp. 106–112, November 2016.

[6] J. M. Hamamreh, E. Guvenkaya, T. Baykas, and H. Arslan, "A Practical Physical-Layer Security Method for Precoded OSTBC-Based Systems," in *IEEE Wireless Commun. Netw. Conf. (WCNC)*, Apr. 2016, pp. 1–6.

[7] Y. Rahmatallah and S. Mohan, "Peak-To-Average Power Ratio Reduction in OFDM Systems: A Survey And Taxonomy," *IEEE Commun. Surv. Tut.*, vol. 15, no. 4, pp. 1567–1592, Fourth 2013.